

Supplementary Materials for

**HDAC5 loss impairs RB repression of pro-oncogenic genes and confers
CDK4/6 inhibitor resistance in cancer**

Yingke Zhou, Xin Jin, Jian Ma, Donglin Ding, Zhenlin Huang, Haoyue Sheng, Yuqian Yan,
Yunqian Pan, Ting Wei, Liguang Wang, Heshui Wu and Haojie Huang

The file includes:

- Supplementary Materials and Methods
- Supplementary References
- Supplementary Table S1. Sequence of gene specific shRNAs
- Supplementary Table S2. Sequence of primers for RT-qPCR and ChIP-qPCR
- Supplementary Table S3. Information of antibodies
- Supplementary Table S4. Information of chemicals
- Supplementary Table S5. Information of cell lines and recombinant DNA
- Supplementary Table S6. QC metrics of RNA-seq data
- Supplementary Table S7. Basic characteristics of ChIP-seq data
- Supplementary Table S8. Top 20 enriched pathways identified by GSEA analysis
- Supplementary Fig. S1. Expression of HDAC family members in the TCGA PRAD database and the effect of HDAC4 and HDAC5 dual inhibitor on PCa cell sensitivity to Palbociclib
- Supplementary Fig. S2. The effect of HDAC5 deficiency on breast cancer cell sensitivity to Palbociclib
- Supplementary Fig. S3. CDK4/6 phosphorylation of RB on S249/T252 impedes RB-N interaction with HDAC5
- Supplementary Fig. S4. CDK2 phosphorylation of RB on T821 dampens RB-C interaction with HDAC5
- Supplementary Fig. S5. HDAC5 is essential for Palbociclib-induced deacetylation on H3K27
- Supplementary Fig. S6. RB-HDAC5 regulate H3K27-ac in an E2F1 dependent manner

Supplementary Materials and Methods

RNA-seq and data analysis

After transfected with control shRNA or shHDAC5 and puromycin selection, PC-3 cells were treated with DMSO (1:1000 v/v dilutions) or Palbociclib (5 μ M) for 24 h. Total RNA was isolated from cells using the RNeasy Plus Mini Kit (QIAGEN). High-quality (Agilent Bioanalyzer RIN > 9) total RNA was employed for the preparation of sequencing libraries using the Illumina TruSeq RNA Library Prep Kit v2. A total of 500–1,000 ng of riboRNA-depleted total RNA was fragmented by RNase III (1.5 unit for 1000 ng RNA) treatment at 37 °C for 10–18 min, and RNase III was inactivated at 65 °C for 10 min. Size selection (50- to 150-bp fragments) was performed using the FlashPAGE denaturing PAGE fractionator (Thermo Fisher Scientific) before ethanol precipitation overnight. The resulting RNA was directionally ligated, reverse-transcribed and treated with RNase H. Samples with biological triplicates were sequenced using the Illumina HiSeq4000 platform at the Mayo Clinic Medical Genome Facility. Pre-analysis quality control was performed using FastQC (<http://www.bioinformatics.babraham.ac.uk/projects/fastqc/>) and RSeQC software (1). Pair-end raw reads were aligned to the human reference genome (GRCh38/hg38) using Tophat (2). Genome-wide coverage signals were represented in BigWig format to facilitate convenient visualization using the UCSC genome browser. Gene-wise raw fragment counts were estimated using HTSeq (3). EdgeR (4) was used to identify differentially expressed genes in different groups using the raw counts as input. Heatmap of differentially expressed genes was generated using RPKM (Reads Per Kilo-base exon per Million mapped reads) as described previously (5). BAM files and the processed data have been deposited into NCBI Gene Expression Omnibus

with accession number GSE155004. The QC metrics of raw RNA-seq data are provided in Supplementary Table S6

Chromatin immunoprecipitation sequencing (ChIP-seq) and data analysis and ChIP-qPCR

ChIP-seq libraries were prepared using the methods as described previously (6) and high throughput sequencing was performed using the Illumina HiSeq4000 platform at the Mayo Clinic Medical Genome Facility. The data were analyzed using the following pipeline: ChIP-seq raw reads were aligned to the human reference genome (GRCh38/hg38) using Bowtie2 (2.2.9), and uniquely mapped reads were kept for further analysis. Peak calling was performed using MACS2 (v2.2.4) with q-value threshold of 0.05, the input controls from PC-3 (GSM2052192) were used to normalize the ChIP seq data. BigWig files were generated for visualization with the UCSC genome browser or IGV. We used GREAT (<http://bejerano.stanford.edu/great/public/html/>) to assign peaks to their potential target genes (a peak-gene association is determined if the peak falls into 2 kb region centering on the transcription start site of the gene) (7). Diffbind (<https://www.bioconductor.org/packages/release/bioc/html/DiffBind.html>) was used to identify significantly differential peaks of H3K27-ac (FDR < 0.05) between the two groups with each group having two biological replicates (replicates were used to calculate p-value and FDR). Then the putative target genes of differential peaks were identified using the GREAT algorithm (<http://great.stanford.edu/public/html/>). Raw and processed data have been deposited into NCBI Gene Expression Omnibus with accession number GSE155004. For ChIP-qPCR experiments, DNA pulled down by antibodies or non-specific IgG were amplified by real-time PCR. Sequence

information for ChIP primers is provided in Supplementary Table S2. The information of ChIP-seq data such as sequencing depths of samples is provided in Supplementary Table S7.

Supplementary References

1. Wang L, Wang S, Li W. RSeQC: quality control of RNA-seq experiments. *Bioinformatics*. 2012;28(16):2184-5.
2. Trapnell C, Pachter L, Salzberg SL. TopHat: discovering splice junctions with RNA-Seq. *Bioinformatics*. 2009;25(9):1105-11.
3. Anders S, Pyl PT, Huber W. HTSeq--a Python framework to work with high-throughput sequencing data. *Bioinformatics*. 2015;31(2):166-9.
4. Robinson MD, Oshlack A. A scaling normalization method for differential expression analysis of RNA-seq data. *Genome Biol*. 2010;11(3):R25.
5. Mortazavi A, Williams BA, McCue K, Schaeffer L, Wold B. Mapping and quantifying mammalian transcriptomes by RNA-Seq. *Nat Methods*. 2008;5(7):621-8.
6. Boyer LA, Lee TI, Cole MF, Johnstone SE, Levine SS, Zucker JP, et al. Core transcriptional regulatory circuitry in human embryonic stem cells. *Cell*. 2005;122(6):947-56.
7. McLean CY, Bristor D, Hiller M, Clarke SL, Schaar BT, Lowe CB, et al. GREAT improves functional interpretation of cis-regulatory regions. *Nat Biotechnol*. 2010;28(5):495-501.

Supplementary Table S1. Sequence of gene-specific shRNAs

shRNAs	Sequence
sh-HDAC1-1	CCGGCGTTCTTAACTTTGAACCATACTCGAGTATGGTTCAAAGTTAA GAACGTTTTT
sh-HDAC1-2	CCGGGCCGGTCATGTCCAAAGTAATCTCGAGATTACTTTGGACATGA CCGGCTTTTT
sh-HADC2-1	CCGGCAGTCTCACCAATTTTCAGAACTCGAGTTTCTGAAATTGGTGA GACTGTTTTT
sh-HADC2-2	CCGGCCAGCGTTTGATGGACTCTTTCTCGAGAAAGAGTCCATCAAAC GCTGGTTTTT
sh-HADC3-1	CCGGCCTTCCACAAATACGGAAATTCTCGAGAATTTCCGTATTTGTG GAAGGTTTTT
sh-HADC3-2	CCGGCGGTCTCTATAAGAAGATGATCTCGAGATCATCTTCTTATAGA GACCGTTTTT

sh-HADC4-1	CCGGCGACTCATCTTGTAGCTTATTCTCGAGAATAAGCTACAAGATG AGTCGTTTTT
sh-HADC4-2	CCGGGCAGCTCAAGAACAAGGAGAACTCGAGTTCTCCTTGTTCTTGA GCTGCTTTTT
sh-HADC5-1	CCGGGACTGTTATTAGCACCTTTAACTCGAGTTAAAGGTGCTAATAA CAGTCTTTTT
sh-HADC5-2	CCGGGCTAGAGAAAGTCATCGAGATCTCGAGATCTCGATGACTTTCT CTAGCTTTTT
sh-HADC6-1	CCGGCATCCCATCCTGAATATCCTTCTCGAGAAGGATATTCAGGATG GGATGTTTTT
sh-HADC6-2	CCGGGCCTACGAGTTTAACCCAGAACTCGAGTTCTGGGTAAACTCG TAGGCTTTTT
sh-HADC7-1	CCGGTCCACACAGAAATGTGAACTTCTCGAGAAGTTCACATTTCTGT GTGGATTTTT
sh-HADC7-2	CCGGGCTGATCTATGACTCGGTCATCTCGAGATGACCGAGTCATAGA TCAGCTTTTT
sh-HADC8-1	CCGGTGACAGAAAGAGATCAGGTTTCTCGAGAAACCTGATCTCTTTC TGTCATTTTT
sh-HADC8-2	CCGGGCATTCTTTGATTGAAGCATACTCGAGTATGCTTCAATCAAAG AATGCTTTTT
sh-HADC9-1	CCGGCGCATTCTAATTCATGAAGATCTCGAGATCTTCATGAATTAGA ATGCGTTTTT
sh-HADC9-2	CCGGGCAAAGATTTAGCTCCAGGATCTCGAGATCCTGGAGCTAAATC TTTGCTTTTT
sh-HADC10-1	CCGGCACCGCAGAAATGACACCGCACTCGAGTGCGGTGTCATTTCTG CGGTGTTTTT
sh-HADC10-2	CCGGCCTGTACCTCTTAGATGGGATCTCGAGATCCCATCTAAGAGGT ACAGGTTTTT
sh-HADC11-1	CCGGGCGCTATCTTAATGAGCTCAACTCGAGTTGAGCTCATTAAAGAT AGCGCTTTTT

sh-HADC11-2	CCGGCTCGCCATCAAGTTTCTGTTTCTCGAGAAACAGAAACTTGATG GCGAGTTTTT
sh-RB1-1	CCGGGTGCGCTCTTGAGGTTGTAATCTCGAGATTACAACCTCAAGAG CGCACTTTTTG
sh-RB1-2	CCGGCAGAGATCGTGTATTGAGATTCTCGAGAATCTCAATACACGAT CTCTGTTTTG
sh-E2F1-1	CCGGCGCTATGAGACCTCACTGAATCTCGAGATTCAGTGAGGTCTCA TAGCGTTTTG
sh-E2F1-2	CCGGCGTGGACTCTTCGGAGAACTTCTCGAGAAGTTCTCCGAAGAGT CCACGTTTTG

Supplementary Table S2. Sequence of primers for RT-qPCR and ChIP-qPCR

Gene	Usage	Forward	Reverse
<i>NCAPG</i>	RT-qPCR	TTAAGGAGGCCTTTCGGCTG	TCCACAGCTGGTTCACGTTT
<i>KIF11</i>	RT-qPCR	TGGCTGACAAGAGCTCAAGG	GGCCATACGCAAAGATAGTGC
<i>CLSPN</i>	RT-qPCR	ATCATCAGCAGTTGGGCCAC	TGAAGCTTTTCACCTCTGTTGG
<i>CENPF</i>	RT-qPCR	AGCCAGACTCTTCCACAAGC	GGGTCTTCTCTTGCTGCCAT
<i>HDAC5</i>	RT-qPCR	CTGCGGAACAAGGAGAAGAG	GGGAACTCTGGTCCAAAGAA
<i>RBI</i>	RT-qPCR	TTTCTGCTTTTGCATTCGTG	GGAAGCAACCCTCCTAAACC
<i>GAPDH</i>	RT-qPCR	ACCCAGAAGACTGTGGATGG	TTCAGCTCAGGGATGACCTT
<i>NCAPG</i> promoter	ChIP-qPCR	TTGTTACCTTCGCGACTCA	AAGGAATAACGGTCCACGCC
<i>KIF11</i> promoter	ChIP-qPCR	GGGCTGACAGGATTCCGAG	CAGCAACCGGGTGTCATTTTT
<i>CLSPN</i> promoter	ChIP-qPCR	ACCCAGATGGTTTGCACCAA	GCCAACTCAGCCTGGGTAAT
<i>CENPF</i> promoter	ChIP-qPCR	TTTTTGCCGGCGGGTACT	GTGAGTCCGTGACCGAGTAG

Supplementary Table S3. Information of antibodies

Antibodies	Source	Identifier
Mouse monoclonal anti-RB	BD Biosciences	Cat# 554136; RRID: AB_395259
Rabbit polyclonal anti-p107	Santa Cruz	Cat# sc-318; RRID: AB_2175428
Rabbit polyclonal anti-p130	Santa Cruz	Cat# sc-317; RRID: AB_632093
Rabbit polyclonal anti-E2F-1	Santa Cruz	Cat# sc-193; RRID: AB_631394
Rabbit polyclonal anti-E2F-2	Santa Cruz	Cat# sc-632; RRID: AB_2277708
Rabbit polyclonal anti-HDAC5	Cell Signaling Technology	Cat# 20458S; RRID: AB_2713973
Mouse monoclonal anti-ERK2	Santa Cruz	Cat# sc-135900; RRID: AB_2141283
Mouse monoclonal anti-FLAG M2	Sigma-Aldrich	Cat# F-3165; RRID: AB_259529
Mouse monoclonal anti-HA.11	Covance	Cat# MMS-101R; RRID: AB_291262
Peroxidase IgG Fraction Monoclonal Mouse Anti-Rabbit IgG	Jackson ImmunoResearch	Cat# 211-032-171; RRID: AB_2339149
Peroxidase AffiniPure Goat Anti- Mouse IgG	Jackson ImmunoResearch	Cat# 115-035-174; RRID: AB_2338512
Rabbit monoclonal anti- Phospho- Rb (Ser249,T252)	Thermo Fisher Scientific	Cat# 701059; RRID: AB_2532363
Mouse monoclonal anti- Phosphoserine/threonine	BD Biosciences	Cat# 612548; RRID: AB_399843

Rabbit monoclonal anti- Acetyl Histone H3 (Lys27)	Cell Signaling Technology	Cat# 8173S; RRID: AB_10949503
Rabbit monoclonal anti- Acetyl Histone H3 (Lys27)	Abcam	Cat# ab4729, RRID:AB_2118291
Rabbit monoclonal anti-beta-Tubulin	Cell Signaling Technology	Cat# 2128; RRID: AB_823664
Rabbit monoclonal anti- Phospho-Rb (Thr821)	Thermo Fisher Scientific	Cat# 44-582G; RRID: AB_2533685
Rabbit monoclonal anti- V5 tag	Abcam	Cat# ab9116, RRID:AB_307024
Mouse monoclonal anti- Ac Histone H3	Santa Cruz	Cat# sc-56616, RRID:AB_2263811
Mouse monoclonal anti- Ac Histone H4	Santa Cruz	Cat# sc-377520
Rabbit monoclonal anti- Histone H3	Abcam	Cat# ab1791, RRID:AB_302613
Rabbit monoclonal anti- Ac Histone H4(Lys16)	Cell Signaling Technology	Cat# 13534S; RRID: AB_2687581
Mouse monoclonal anti- Histone H4	Santa Cruz	Cat# sc-25260, RRID:AB_2118623
Rabbit monoclonal anti- BRD4	Abcam	Cat# ab128874, RRID:AB_11145462

Supplementary Table S4. Information of chemicals

Chemicals	Source	Identifier
Palbociclib	Selleckchem	Cat# S1116
Temsirolimus	AbMole BioScience	Cat# M3722
VE822	TargetMol	Cat# 1232416-25-9
JQ1	Sigma-Aldrich	Cat# SML1524
Olaparib	Selleckchem	Cat# S1060
GSK126	TargetMol	Cat# T2079
GDC0068	MedChemExpress	Cat# HY-15186A
I-CBP112	Cayman	Cat# 14468
JSH-23	Millipore	Cat# 481408
Vorinostat	Cayman	Cat# 10009929-500
Propidium Iodide	Thermo Fisher	Cat# P1304MP
Flavopiridol hydrochloride hydrate	Sigma-Aldrich	Cat# F3055
Roscovitine	MedChemExpress	Cat# HY-30237
TMP195	Cayman	Cat# 23242
RGFP966	MedChemExpress	Cat# HY-13909
Tubastatin A	Sigma-Aldrich	Cat# SML0044
NEO2734(ep06)	NEO Med Institute (from Dr. Bill Brown)	N/A
LMK235	Cayman	Cat# 14969

Supplementary Table S5. Information of cell lines and recombinant DNA

Cell line	Source	Identifier
Human: C4-2	ATCC	N/A
Human: PC-3	ATCC	CRL-1435
Human: HEK293T	ATCC	CRL-11268
Recombinant DNA	Source	Identifier
pCMV-HA-hRB-WT	Addgene	Cat# 58905
pCMV-HA-hRB Δ CDK	Addgene	Cat# 58906
pcDNA3.1-Flag-hHDAC5-WT	Addgene	Cat# 32213

Supplementary Table S6. QC metrics of RNA-seq data

samples	total reads	mapped reads	mapped ratio	uniquely mapped	unique ratio	unmapped reads	unmapped ratio
shNC+DMSO#1	60940456	52570154	0.862648	42967056	0.705066	8370302	0.137352
shNC+DMSO#2	59783602	55914070	0.935274	45552154	0.761951	3869532	0.064726
shNC+DMSO#3	65149244	55159962	0.846671	45048120	0.69146	9989282	0.153329
shNC+Palbo#1	66107994	58900922	0.89098	48317322	0.730885	7207072	0.10902
shNC+Palbo#2	71493540	63850842	0.893099	52349910	0.732233	7642698	0.106901
shNC+Palbo#3	78775774	72914000	0.925589	59692094	0.757747	5861774	0.074411
shHDAC5+DMSO#1	64076146	61136248	0.954119	51101248	0.797508	2939898	0.045881
shHDAC5+DMSO#2	58368162	54224838	0.929014	45476232	0.779127	4143324	0.070986
shHDAC5+DMSO#3	58817334	54938268	0.934049	46049306	0.782921	3879066	0.065951
shHDAC5+Palbo#1	75937278	70662494	0.930538	59021388	0.777239	5274784	0.069462
shHDAC5+Palbo#2	62151746	58612684	0.943058	49023030	0.788764	3539062	0.056942
shHDAC5+Palbo#3	50883128	48084020	0.944989	40098030	0.788042	2799108	0.055011

Supplementary Table S7. Basic characteristics of ChIP-seq data

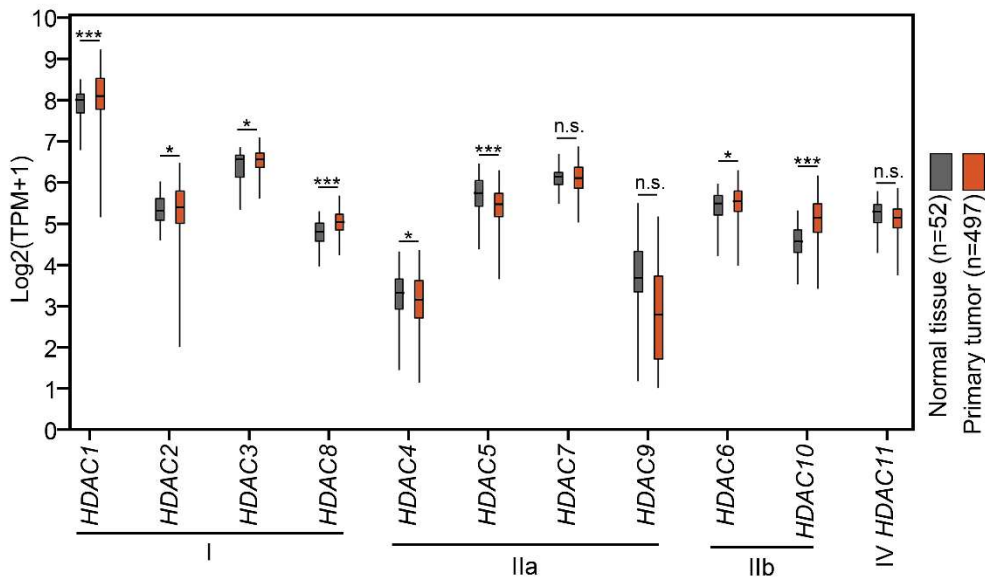
	PC-3_DMSO- 1_H3K27Ac	PC-3_DMSO- 2_H3K27Ac	PC-3_Palbociclib- 1_H3K27Ac	PC-3_Palbociclib- 2_H3K27Ac
Total reads	31489274	33842826	28638686	28172860
Mapped reads	30639963	32872469	27748432	27247540
Mapped ratio	0.973028562	0.971327542	0.968914286	0.967155624
Uniquely mapped	28329711	30447476	25677848	25244179
Unique ratio	0.899662247	0.899672976	0.896614042	0.896046017
Unmapped reads	849311	970357	890254	925320
Unmapped ratio	0.026971438	0.028672458	0.031085714	0.032844376

Supplementary Table S8. Top 20 enriched pathways in GSEA analysis

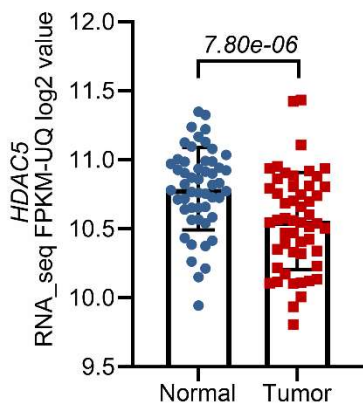
Name	SIZE	ES	NES	NOM p-val	FDR q-val	FWE R p-val
GO MITOTIC CELL CYCLE	26	0.7789 42	1.7233 29	0	0.0262 88	0.02 8
GO REGULATION OF MITOTIC CELL CYCLE	14	0.8082 6	1.6976 02	0	0.0239 84	0.05
GO CELL CYCLE	29	0.7586 32	1.6723 08	0	0.0313 39	0.09 4
GO CELL CYCLE PROCESS	25	0.7598 11	1.6674 63	0.0010 04	0.0272 55	0.11
GO REGULATION OF CELL CYCLE PROCESS	14	0.7751 33	1.6460 77	0.0010 12	0.0327 25	0.16 1
GO REGULATION OF CELL CYCLE	18	0.7549 09	1.6234 19	0.0010 07	0.0453 7	0.24 8
GO_REGULATION_OF_CELL_CYCLE_PHASE_TRANSITION	11	0.7802 47	1.5980 55	0	0.0651 49	0.37 5
GO CELL CYCLE PHASE TRANSITION	13	0.7417 88	1.5612 62	0.0040 77	0.1150 19	0.60 4
GO CELL CYCLE G2 M PHASE TRANSITION	9	0.7706 27	1.5385 39	0.0093 56	0.1562 15	0.77 2
GO REGULATION OF CELL DEVELOPMENT	6	0.8248	1.5338 33	0.0098 15	0.1517 24	0.79 6
GO_POSITIVE_REGULATION_OF_TRANSFERASE_ACTIVITY	6	0.8202 46	1.5316 77	0.0098 9	0.1433 4	0.81
GO_REGULATION_OF_CELL_CYCLE_G2_M_PHASE_TRANSITION	9	0.7706 27	1.5315 75	0.0063 09	0.1319 49	0.81 1
GO MITOTIC CELL CYCLE CHECKPOINT	4	0.8833 33	1.5161 41	0.0133 98	0.1572 2	0.87 8
GO DNA PACKAGING	6	0.8199 13	1.5093 09	0.0120 61	0.1624 02	0.90 5
GO DNA METABOLIC PROCESS	15	0.7164 68	1.5073 91	0.0080 81	0.1562 9	0.91
GO NEGATIVE REGULATION OF CELL CYCLE	10	0.7437 4	1.5073 85	0.0072 16	0.1465 22	0.91
GO_REGULATION_OF_NERVOUS_SYSTEM_DEVELOPMENT	5	0.8418 59	1.5038 67	0.0123 73	0.1457 56	0.91 8
GO TAXIS	3	0.9382 05	1.4977 5	0.0080 86	0.1517 64	0.93 1
GO CYTOKINE PRODUCTION	4	0.8736 66	1.4866	0.0189 8	0.1703 66	0.96 1
GO EMBRYO DEVELOPMENT	7	0.7753 24	1.4828 14	0.0234 04	0.1716 52	0.97 1

SF1

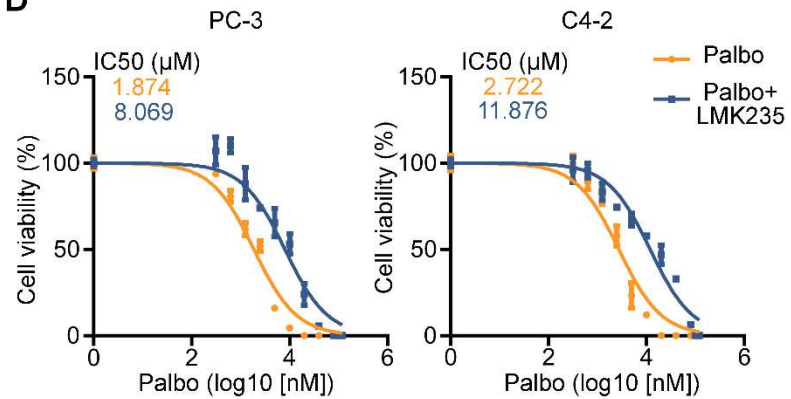
A



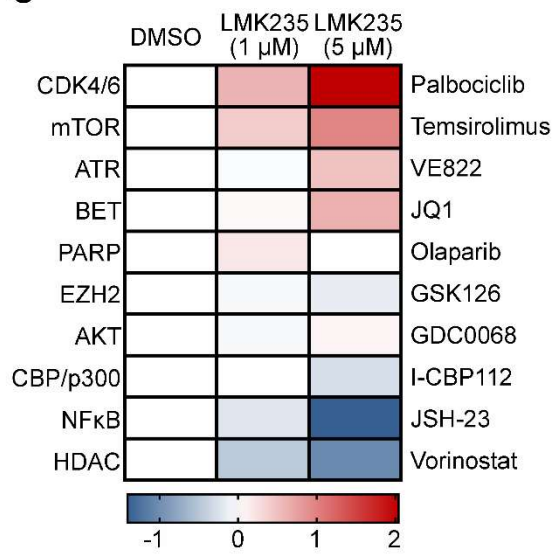
B



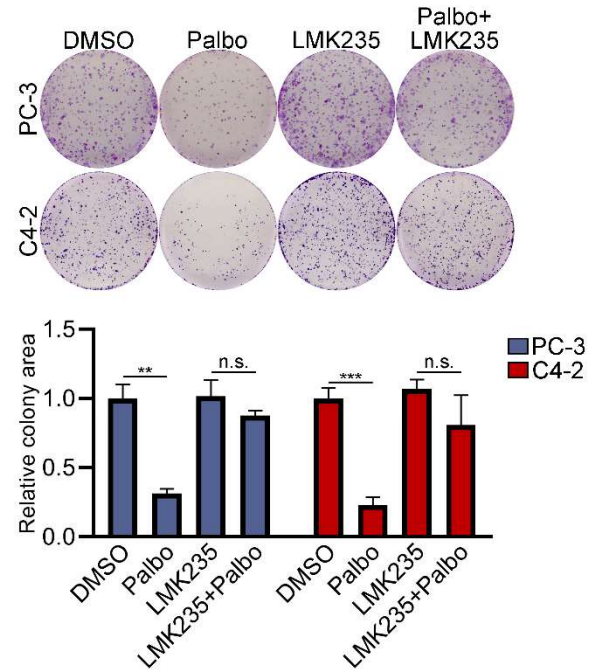
D



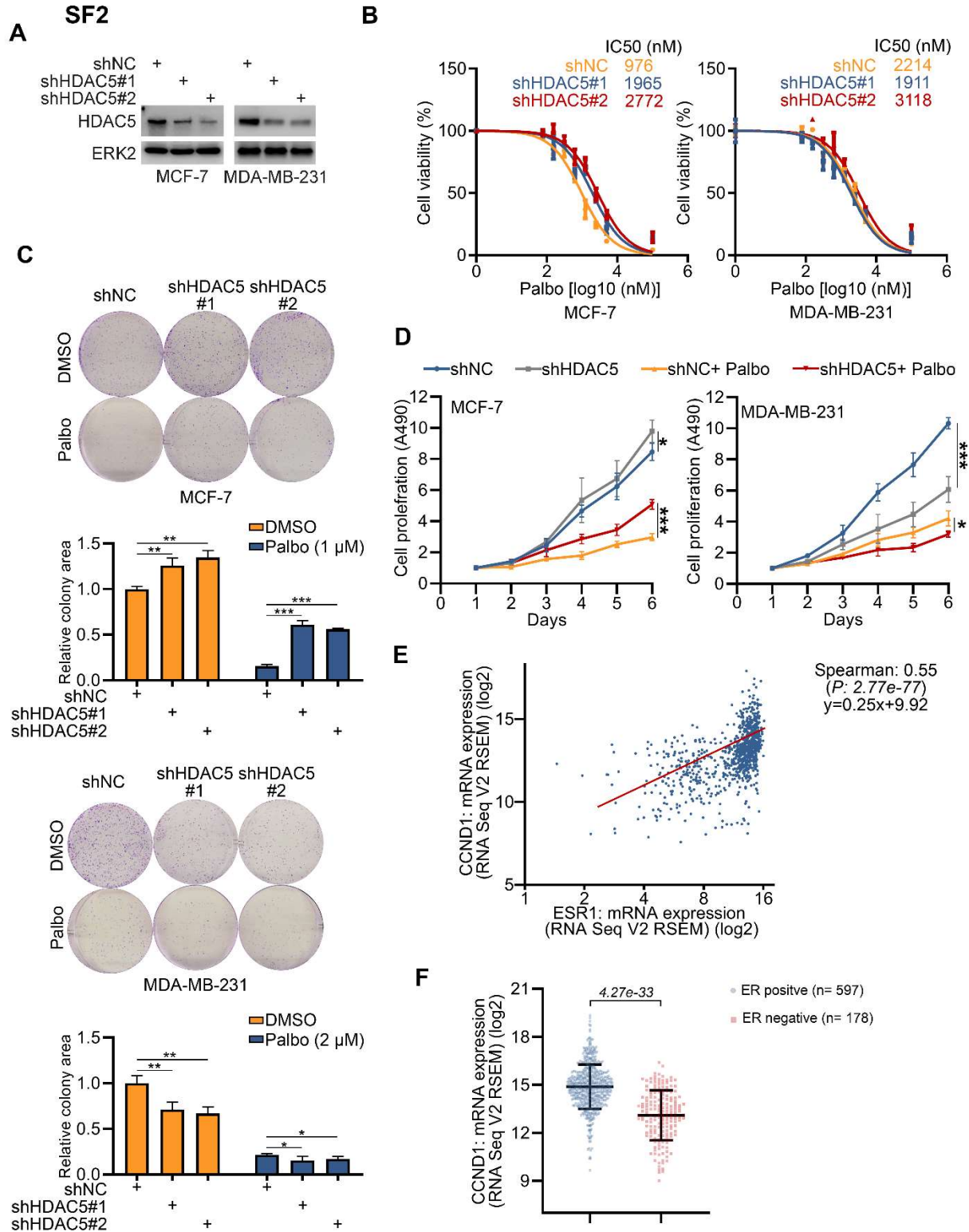
C



E



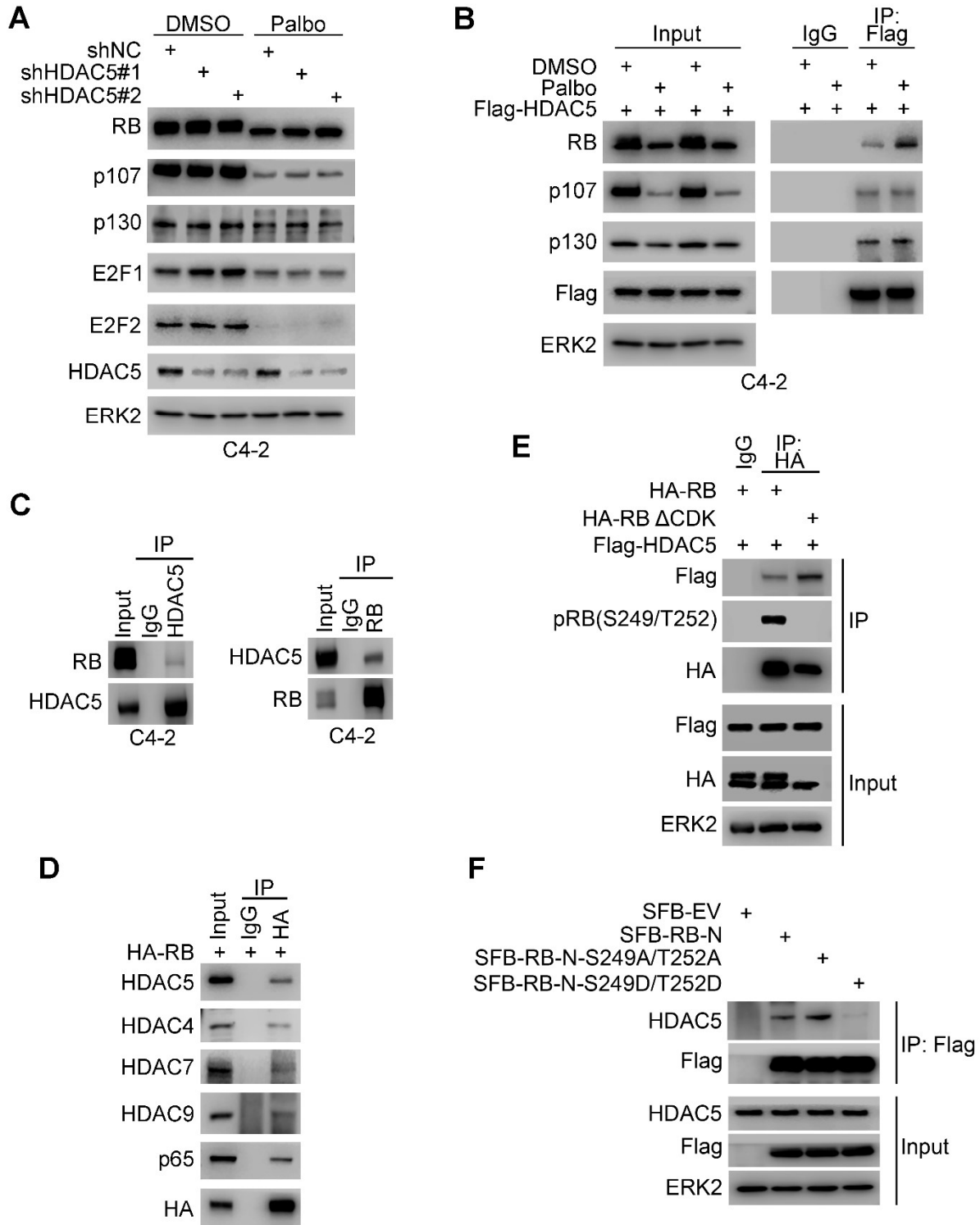
Supplementary Fig. S1. Expression of HDAC family members in the TCGA PRAD database and the effect of HDAC4 and HDAC5 dual inhibitor on PCa cell sensitivity to Palbociclib (A) Box plot showing the comparison of mRNA level of 11 HDAC family members (except Sirtuins) between normal and tumor tissues from the TCGA prostate adenocarcinoma (PRAD) database. *P* values were determined between normal tissues (*n* = 52) and tumor tissues (*n* = 497) for each gene by Wilcoxon rank sum test with continuity correction. n.s., not significant; **P*<0.05; ** *P*<0.01; *** *P*<0.001. (B) Column plot showing the mRNA level of *HDAC5* gene between paired normal and tumor tissues for individual patient from the TCGA PRAD database (*n* = 52). (C) Heatmap shows the normalized IC₅₀ ratio (log₂ [IC₅₀ ratio]) of indicated inhibitors in PC-3 cells treated with vehicle (DMSO) or LMK235 as revealed by MTS assay. (D) PC-3 or C4-2 cells were treated with DMSO (1:1000 v/v dilutions) or 5 μM LMK235 and were further treated with different doses with Palbociclib for 48 h and cell viability was measured by MTS assay. (E) PC-3 and C4-2 cells were treated with indicated drugs (LMK235, 5 μM; Palbociclib, 5 μM) and used for colony formation assay. Colonies was quantified using ImageJ. Data are shown as mean ± SD (*n*=3). n.s., not significant; ** *P*<0.01; *** *P*<0.001.



Supplementary Fig. S2. The effect of HDAC5 deficiency on breast cancer cell sensitivity to Palbociclib. (A) MCF-7 and MDA-MB-231 breast cancer cell lines were infected with lentivirus expressing non-specific control (shNC) or HDAC5-specific shRNAs (shHDAC5) for 48 h and cells were harvested for western blot analysis. ERK2 was used as a loading control. (B) Control

or HDAC5 knockdown MCF-7 and MDA-MB-231 cells were treated with Palbociclib in different doses for 48 h and cell viability was measured by MTS assay. (C) Control or HDAC5 knockdown MCF-7 and MDA-MB-231 cells were seeded in 6-well plates for colony formation assay. 7 days after treatment with vehicle (DMSO) or Palbociclib (1 μ M for MCF-7, 2 μ M for MDA-MB-231), colonies were stained by violet blue and photographed and quantified using ImageJ. Data are shown as mean \pm SD (n=3). * P <0.05; ** P <0.01; *** P <0.001. (D) Control or HDAC5 knockdown MCF-7 and MDA-MB-231 cells were treated with indicated drugs (1 μ M of Palbociclib for MCF-7 and 2 μ M of Palbociclib for MDA-MB-231). Cell proliferation rate was measured over a time course. Data are shown as mean \pm SD (n = 6). * P <0.05; *** P <0.001. (E) Analysis of correlation of mRNA level (RNA Seq V2 RSEM, log₂) between *ESR1* and *CCND1* genes in the TCGA breast cancer database. (F) Box plot of mRNA level (RNA Seq V2 RSEM, log₂) of *CCND1* in ER-positive and ER-negative patient samples in the TCGA breast cancer database.

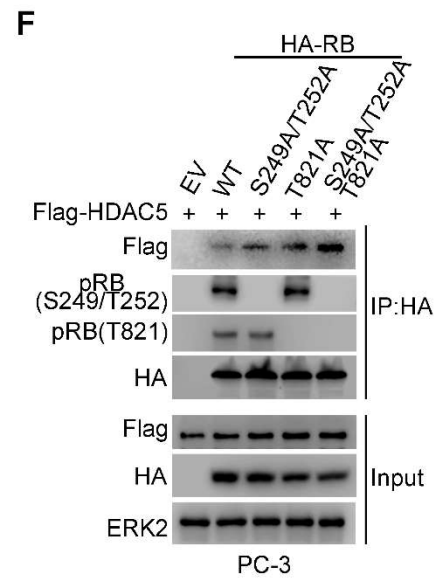
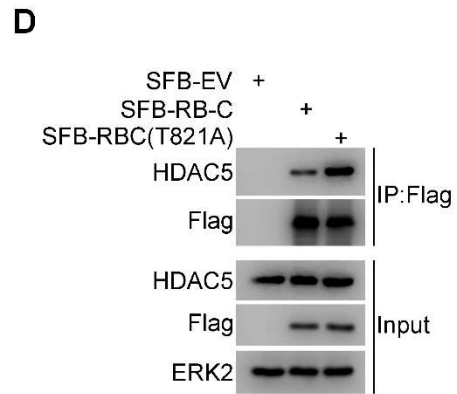
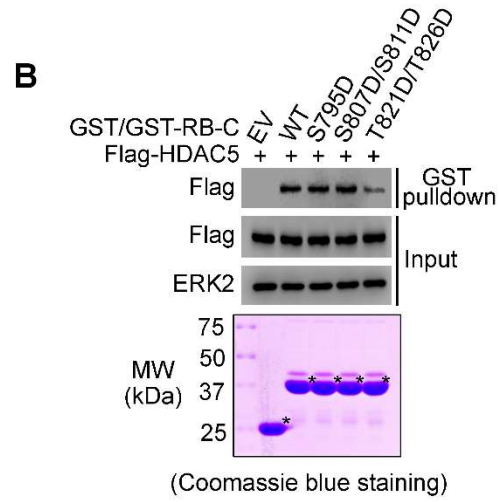
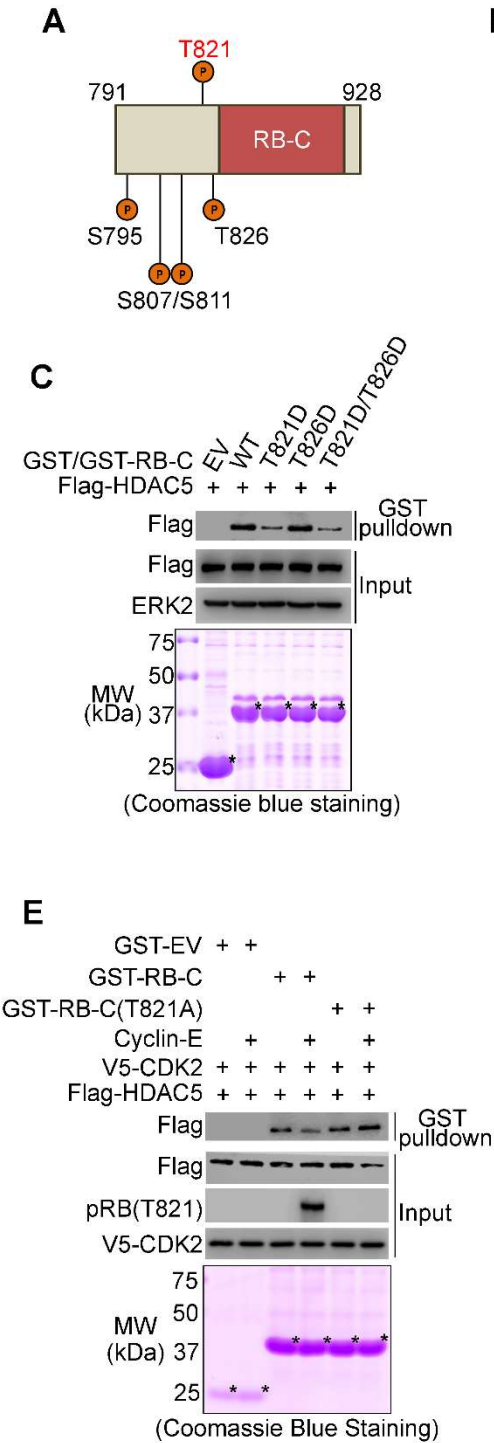
SF3



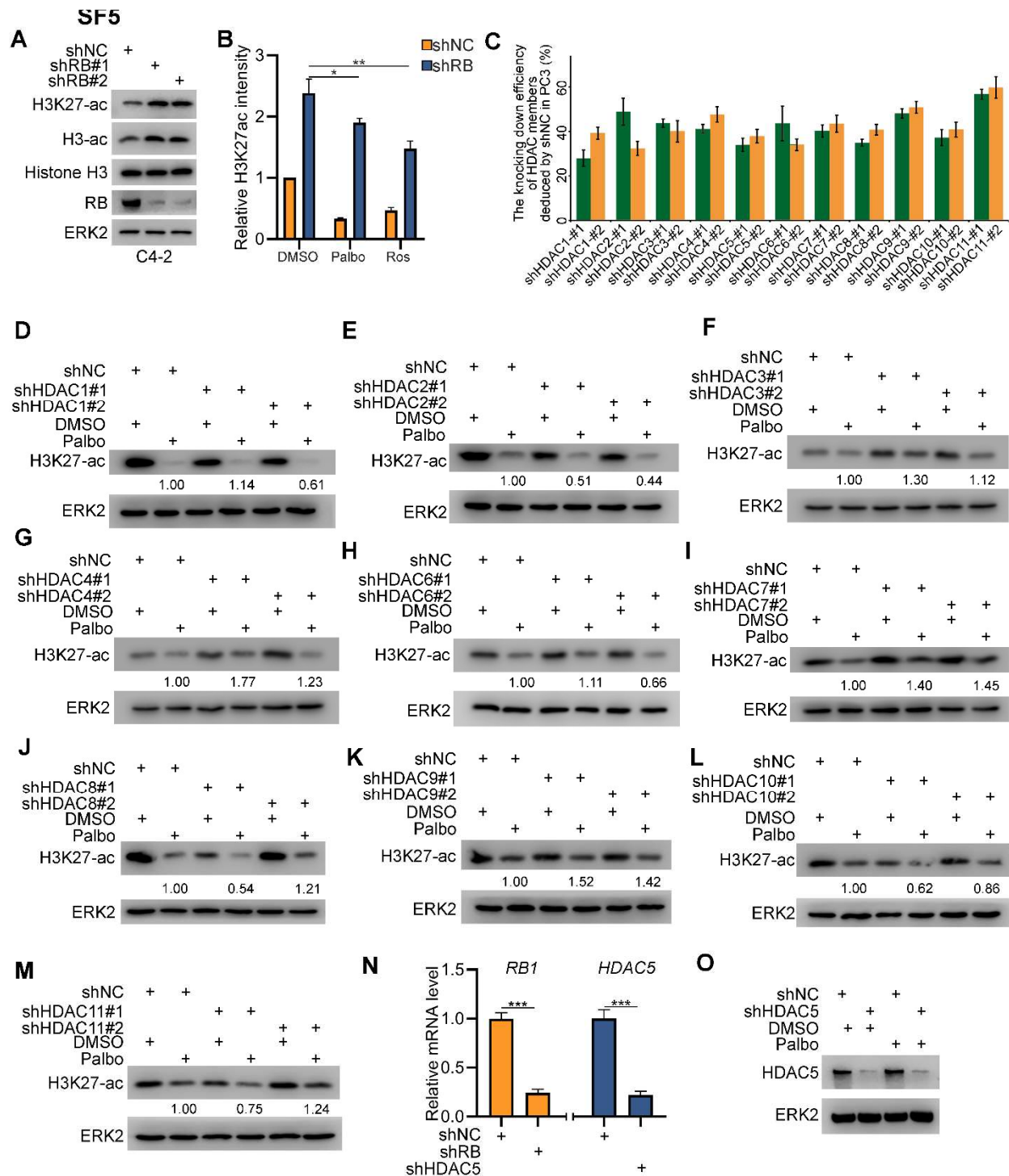
Supplementary Fig. S3. CDK4/6 phosphorylation of RB onS249/T252 impedes RB-N

interaction with HDAC5. (A) C4-2 cells infected with lentivirus expressing control or HDAC5 specific shRNAs for 48 h and treated with DMSO or Palbociclib (5 μ M) for 24 h followed by and western blot analysis. (B) C4-2 cells were transfected with indicated plasmids for 24 h treated with DMSO or Palbociclib (5 μ M) for 24 h followed by coIP and western blot analyses. (C) Reciprocal coIP and western blot analyses of endogenous HDAC5 and RB protein interaction in C4-2 cells. (D-F) CoIP and western blot analysis in 293T cells after transfected with indicated plasmids for 24 h.

SF4

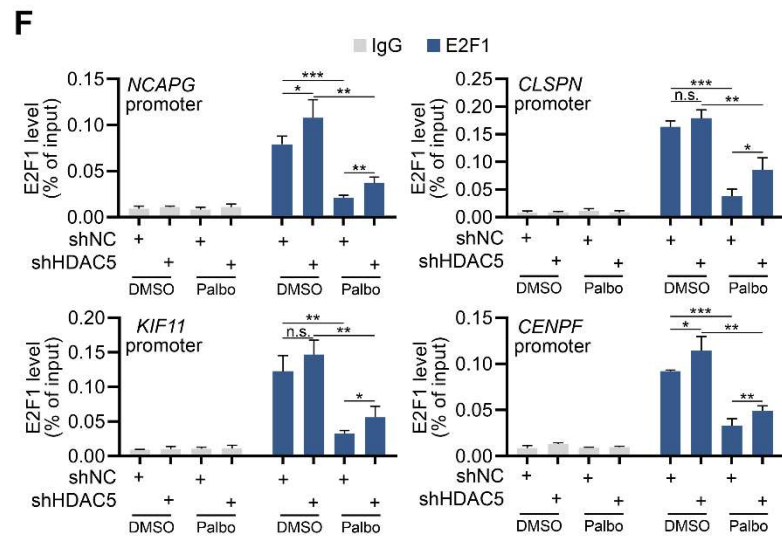
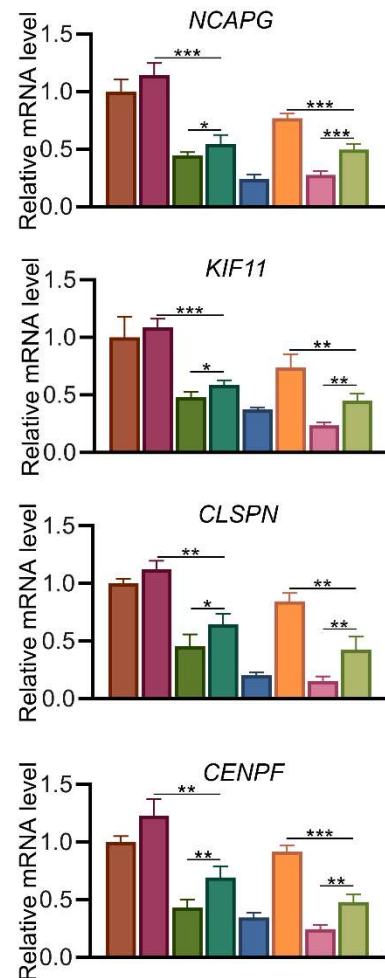
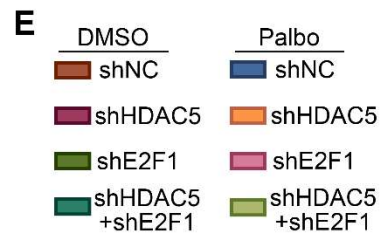
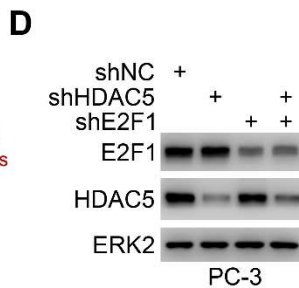
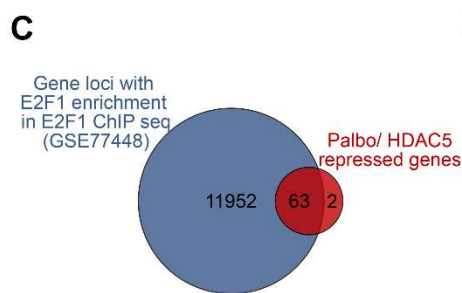
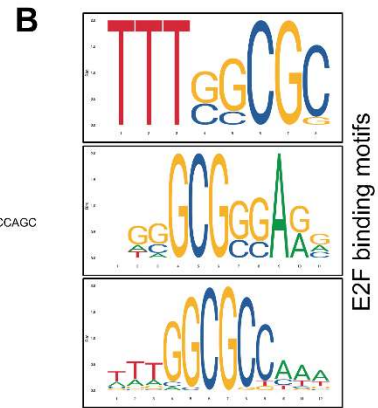
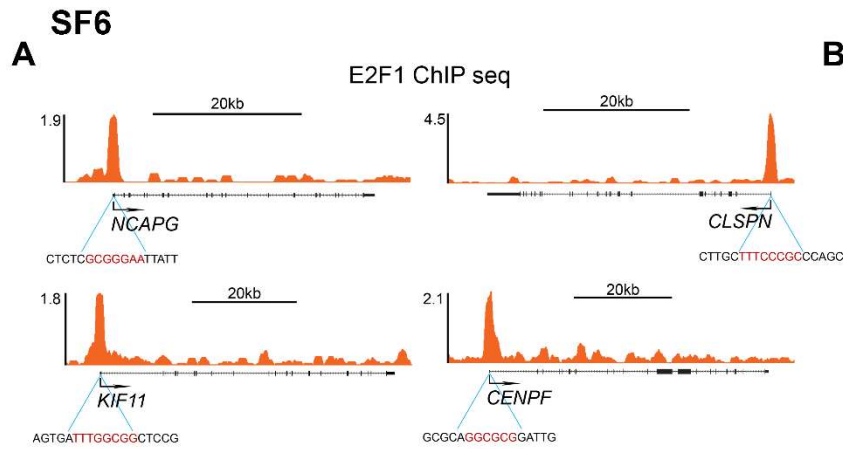


Supplementary Fig. S4. CDK2 phosphorylation of RB on T821 dampens RB-C interaction with HDAC5. (A) Schematic diagram depicting CDK phosphorylation sites on RB-C. (B, C) Western blot analysis of proteins, pulled down by indicated un-mutated (WT) or mutated GST-RB-C recombinant proteins, from whole cell lysate (WCL) of PC-3 cells transfected with Flag-HDAC5. (D) Western blot analysis of WCL and coIP samples from 293T cells transfected with indicated plasmids for 24 h. (E) Western blot analysis of *in vitro* transcribed and translated HDAC5 proteins pulled down by GST-RB-C. GST recombinant proteins were inoculated with purified Cyclin E and CDK2 for *in vitro* kinase assay prior to GST pulldown assay. (F) Western blot analysis of WCL and coIP samples from PC-3 cells at 24 h after transfection with indicated plasmids.



Supplementary Fig. S5. HDAC5 is essential for Palbociclib-induced deacetylation on H3K27. (A) C4-2 cells were infected with indicated shRNAs for 48 h and harvested for western blot analysis. (B) H3K27-ac intensity of western blots in Fig. 4C was quantified using ImageJ and normalized to the value in shNC cells treated with DMSO. Data are shown as mean \pm SD ($n = 2$). * $P < 0.05$; ** $P < 0.01$. (C) PC-3 cells were infected with indicated shRNAs for 48 h and harvested for RT-qPCR. (D-M) PC-3 cells were infected with lentivirus expressing control or gene specific shRNAs as indicated. 48 h after infection, cells were treated with DMSO or

Palbociclib (5 μ M) for 24 h and harvested for western blot analysis. (N) PC-3 cells infected with lentivirus expressing non-specific control (shNC) or gene-specific shRNA as in Figure 4H were harvest for RT-qPCR analysis of *RBI* and *HDAC5* mRNA expression. Data are shown as mean \pm SD (n = 3). *** $P < 0.001$. (O) PC-3 cells were infected with lentivirus expressing non-specific control (shNC) or HDAC5-specific shRNA (shHDAC5) for 48 h. After puromycin selection, cells were treated with DMSO or 5 μ M of Palbociclib for 24 h and were harvested for western blot.



G

	HDAC4	HDAC5	HDAC7	HDAC9
NCAPG	0.225	3.80e-09	0.904	0.333
KIF11	0.587	6.44e-13	3.33e-04	0.5
CLSPN	9.22e-05	5.48e-17	3.93e-03	5.28e-04
CENPF	0.043	1.51e-11	0.597	0.0385

Supplementary Fig. S6. RB-HDAC5 regulates H3K27-ac in an E2F1 dependent manner. (A) UCSC Genome Browser screen shots of E2F1 ChIP-seq (GSE77448) showing E2F1 occupancy in the promoter of the Palbociclib and HDAC5 co-target genes *NCAPG*, *KIF11*, *CLSPN* and *CENPF* in PC-3 cells. (B) Canonical E2F binding motifs defined using JASPAR 2020. (C) Venn diagram shows the overlap between E2F1 target genes and 65 Palbociclib/HDAC5 co-target genes shown in Fig. 5C. (D) PC-3 cells were infected with indicated lentivirus and after 48 h puromycin selection, and cells were harvested for western blot. (E) PC-3 cells were infected with indicated lentivirus and after puromycin selection, cells were treated with DMSO or Palbociclib (5 μ M) for 24 h and harvested for RT-qPCR analysis of *NCAPG*, *KIF11*, *CLSPN* and *CENPF* gene expression. Data are shown as mean \pm SD (n=3). * $P < 0.05$; ** $P < 0.01$; *** $P < 0.001$. (F) ChIP-qPCR analysis of E2F1 occupancy at the promoter of *NCAPG*, *KIF11*, *CLSPN* and *CENPF* genes in PC-3 cells. Cells were infected with lentivirus expressing control or HDAC5 specific shRNAs for 48 h and treated with DMSO or Palbociclib (5 μ M) for 24 h. Data are shown as mean \pm SD (n=3). n.s. not significant; * $P < 0.05$; ** $P < 0.01$; *** $P < 0.001$. (G) Heatmap generated based on the P value of Pearson correlation showing the correlation coefficient between the four Palbociclib/HDAC5 co-target genes and Class IIa HDAC members.